



Momoe Sakamori (DEP/UNICAMP & INCT-GP) and Ricardo Biloti (IMECC/UNICAMP & INCT-GP)

Copyright 2015, SBGf - Sociedade Brasileira de Geofísica.

This paper was prepared for presentation at the 14th International Congress of the Brazilian Geophysical Society, held in Rio de Janeiro, Brazil, August 3-6, 2015.

Contents of this paper were reviewed by the Technical Committee of the 14th International Congress of The Brazilian Geophysical Society and do not necessarily represent any position of the SBGf, its officers or members. Electronic reproduction or storage of any part of this paper for commercial purposes without the written consent of The Brazilian Geophysical Society is prohibited.

Abstract

In migration velocity analysis (MVA), the residual moveout in the image gather is used to estimate velocity update parameters. In this work we propose a numerical approach instead of using approximations to describe the moveout in the image gather considering a dipping reflector. In addition to this, our description is valid for neighbouring image gathers, so that several image gathers can be used simultaneously to obtain the velocity correction and reflector's dip parameters. We use an optimization algorithm to estimate the parameters in some synthetic models.

Introduction

After migration, it is expected that in a common image gather (CIG), the same reflections are imaged to the same depth, so that the events get flattened. However, if the velocity used in migration is wrong, the events have a residual moveout. For a migration velocity lower than the correct one, events curve upward, whereas if the velocity is higher, events curve downward. This moveout can be used to correct the velocity (Sattlegger (1975)). Migration velocity analysis (MVA) is a seismic processing technique that investigates the migration residual moveout to correct an a priori velocity field.

Al-Yahya (1989) proposed a formula that relates the moveout in the image gather with the errors in the velocity model based on a horizontal reflector embedded in a constant velocity overburden. It is used to obtain a velocity correction factor from fitting the theoretical moveout curve to the event observed in the image gather.

Schleicher and Biloti (2007) proposed a generalization of Al-Yahya's formula considering dipping reflectors. During their derivations, they arrived at a 5th-order polynomial that can not be solved analytically. To obtain a solution, they used a Taylor series expansion and further auxiliary approximations. Since Schleicher and Biloti used a Taylor approximation, theoretically their result is valid only for small dips.

We start expanding some calculations to obtain our proposal. Through numerical experiments, we validate our proposal and take some conclusions.

Theory

Migration is a seismic process that maps the reflection event in a seismic trace back to the position that really originated the reflection. If the velocity used in (time) migration is correct, then the reflection events are mapped to the right vertical (time) position. So that, for a common image gather, the reflection events get flattened, since the reflection events related to the same depth point are mapped to the same time position. However, if a wrong velocity is used to migrate the data, then the reflection events are moved to erroneous positions, which generate the moveout in a CIG.

For a horizontal reflector embedded in a homogeneous medium, Al-Yahya (1989) derived the following formula to describe the time-migrated event in a CIG:

$$t_{AV}^2(h) = t_0^2 + (\gamma^2 - 1)4h^2/v_m^2, \quad (1)$$

where h is the half-offset, t_0 is the vertical time and $\gamma = v_m/v$ is the velocity correction factor, representing the ratio between the migration velocity v_m and the true medium velocity v .

Considering a dipping reflector, Schleicher and Biloti (2007) generalized Al-Yahya's formula (1). In the following, we repeat some theoretical derivations of their work that are important to explain our ideas and where they differ from the ideas of previous works.

Figure 1 represents the geometry of a dipping reflector of angle θ , where x_s and x_r are, respectively, source and receiver horizontal position, h is the half-offset, $d = my + z_0$ is the depth of the reflector under the midpoint y and z_0 denoting the depth of the reflector at the origin.

The reflection traveltme for a dipping reflector is given by

$$t_{ref}(y, h) = \frac{2}{v} \frac{r}{\sqrt{1+m^2}} = \frac{2}{v} r \cos \theta, \quad (2)$$

where $m = \tan \theta$ and $r = \sqrt{d^2 + h^2}$.

Given midpoint y and half-offset h , the semi-ellipse in Figure 2 represents all points with the same traveltme from source x_s and receptor x_r . The family of all isochrons is described by

$$t(x; y, h) = \frac{2z}{v_m} = \frac{2b}{v_m} \sqrt{1 - \frac{(x-y)^2}{a^2}}, \quad (3)$$

where x is the horizontal coordinate of the image point, and the half-axes of the ellipse are given by $a = v_m t_{ref}/2$ and $b = \sqrt{a^2 - h^2}$.

Fixing h and varying y , the envelope of the curves given by equation (3) describes the reflection event in the image gather.

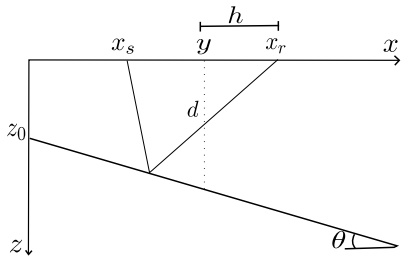


Figure 1: Geometry of a dipping reflector of angle θ , where x_s and x_r are, respectively, source and receiver horizontal position, h is the half-offset, d is the depth of the reflector under the midpoint y and z_0 is the depth of the reflector at origin.

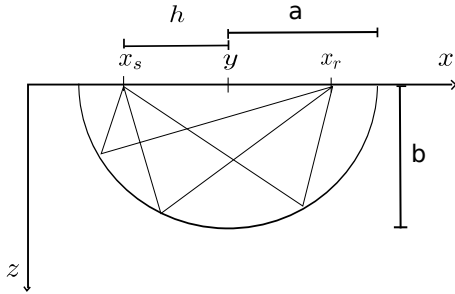


Figure 2: Semi-ellipse of all points with the same traveltime, where x_s and x_r are, respectively, source and receiver horizontal position, h is the half-offset, y is the midpoint, a and b are the half-axes of the ellipse.

Replacing the reflection traveltime (2) into equation (3), we have

$$t(x; y, h) = \frac{2}{v_m} \frac{1}{\gamma \sqrt{1+m^2}} \frac{pq}{r}, \quad (4)$$

where $p = \sqrt{\gamma^2 r^2 - (1+m^2)(x-y)^2}$ and $q = \sqrt{\gamma^2 r^2 - (1+m^2)h^2}$.

The envelope condition is

$$\frac{dt}{dy} = \frac{2}{v_m} \frac{1}{\gamma \sqrt{1+m^2}} \frac{1}{pqr^3} f(x; y, h) = 0, \quad (5)$$

where

$$f(x; y, h) = p^2(1+m^2)h^2m(my+z_0) + q^2r^2 \left[\gamma^2 m(my+z_0) + (1+m^2)(x-y) \right]. \quad (6)$$

This condition defines the midpoint y^* where the reflection associated with the image point x is found in the original data section. After the stationary y^* is obtained, the event location is calculated substituting y^* back into (4). Observe that x is not fixed. Therefore, In Schleicher and Biloti (2007) work, they fixed x , so that their proposal is valid only for a single image gather.

Since f is a polynomial of degree five in y , $f = 0$ can not be solved analytically, except for the particular case of zero-offset. Schleicher and Biloti used Taylor expansion up to fourth order in m around zero to find an approximated solution y for $f = 0$. For doing so, the condition $m \ll 1$ must be fulfilled, which means that their formula is valid for small dips only. Besides, during their derivations, x is fixed equal to zero, so that only one image gather at a time is considered.

In this work we propose to obtain y^* by solving equation (5) numerically. This allows the use of greater dips and gives us a better approximation for the event curve. Another advantage of the numerical solution is that we can solve equation (5) for more than a single image gather, since x is not fixed, extending the work of Schleicher and Biloti.

For an image point x , we find the solution y^* for each h . In general, for an iterative numerical method a reasonable initial guess for y is necessary. As mentioned above, equation (5) can be solved analytically for $h = 0$. The solution is

$$y_0 \equiv y^*(0) = \frac{\gamma^2 m z_0 + (1+m^2)x}{(1-\gamma^2)m^2 + 1}. \quad (7)$$

This value is used as the initial value for the smallest half-offset. Employing a continuation strategy, we then use the solution for the previous h as initial guess for the following offset. After calculating the numerical solution y^* , it is substituted into equation (4) and the moveout surface $t(x; y^*(h), h)$ is obtained.

To calculate the moveout surface, the values of the parameters z_0 , γ and m are required. The search of parameter z_0 is exchanged by calculating the surface for several time samples. This is possible because they are correlated, as we show next.

We estimate the vertical time τ_0 upon substitution of equation (7) into formula (4). This yields

$$\tau_0(x) = \frac{2\gamma(mx+z_0)}{v_m} \frac{1}{\sqrt{|(1-\gamma^2)m^2+1|}}. \quad (8)$$

From this relation, z_0 can be converted in τ_0 and vice versa.

Let us now consider the image gather at \bar{x} , in the vicinity of the image gather at x . In other words, $\bar{x} = x + \delta x$. Substituting \bar{x} into equation (8), the corresponding vertical time reads

$$\tau_0(\bar{x}) = \tau_0(x) + \frac{2}{v_m} \gamma m \delta x \frac{1}{\sqrt{|(1-\gamma^2)m^2+1|}}. \quad (9)$$

To evaluate how good a so-determined theoretical surface fits an actual migrated event, we determine the coherence along the trial surface. The parameters γ and m that describe the best-fitting surface are obtained by maximizing a coherence measure.

In order to search these optimal parameters, we use BOBYQA, (Powell (2009)), an algorithm for bound constrained optimization without derivatives. BOBYQA (Bound Optimization BY Quadratic Approximation) is an algorithm that seeks the minimum of a function $F(u)$, $u \in \mathbb{R}^N$, subject to simple bounds $a \leq u \leq b$. No derivatives of F

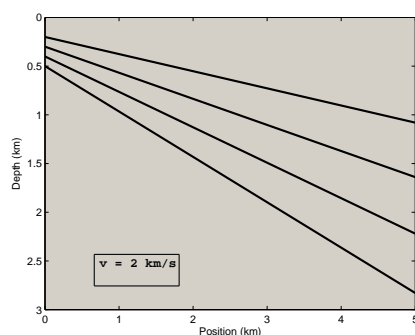


Figure 3: Model of four interfaces with dips of 10° , 15° , 20° and 25° degrees, respectively, embedded in a homogenous medium of velocity 2 km/s.

are required. At each iteration k , it employs a quadratic approximation Q to F that satisfies $Q(\bar{u}_j) = F(\bar{u}_j)$, $j = 1, 2, \dots, M$ where the interpolation points u_j are chosen and adjusted automatically. The typical value for M is $2N + 1$, where N is the problem dimension. In our case, the objective function is the coherence value along the trial surface and the variables of the 2-dimensional problem are γ and m .

The most important parameter for the migration velocity analysis is the velocity correction parameter γ . Once γ is obtained, the velocity field is updated and the data has to be migrated again. Generally, this cycle repeats until the events in the image gathers get flattened, which means that the velocity field updated is good enough.

Numerical examples

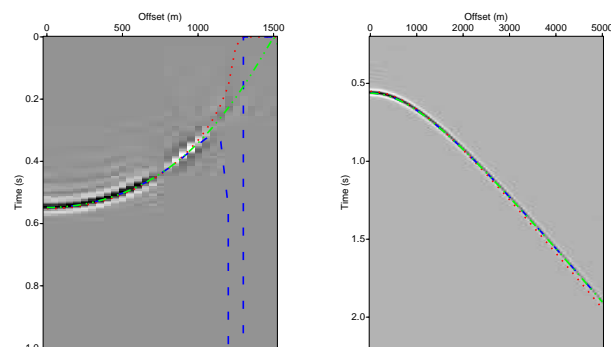
In this section we present some numerical examples. Our model consists of four dipping reflector with increasing dips of 10° , 15° , 20° and 25° , embedded in a homogeneous media of velocity 2 km/s, see Figure 3. The synthetic data is generated by SUSYNLV, a seismic ray-tracing algorithm from Seismic Unix (SU), (Stockwell and Cohen (2008)), with a sampling rate of 4 ms. For the experiment, we simulate 101 midpoints at every 50 m along the seismic profile between 0 and 5 km with 101 source-receiver offsets at every 50 m from 0 up to 5 km.

We conduct three kinds of experiments. In the first one, we validate our proposal by constructing the theoretical curves from the proposals described in the previous section. The second numerical example illustrates the objective function behavior of our proposal using supergatherers. The third part is dedicated to estimating the parameters.

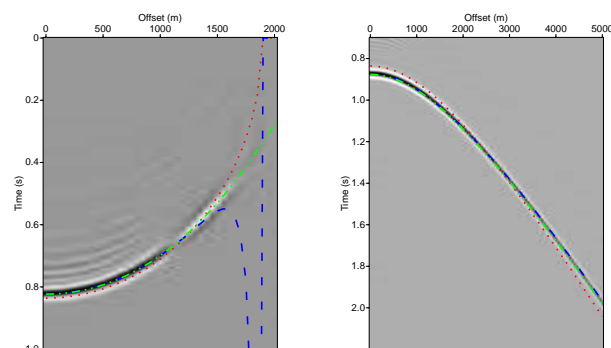
Predicted curves

The objective of this first experiment is to analyse how well our proposal curves describe reflection events in a CIG. For the experiment, we applied Kirchhoff type migration algorithm to the data using a lower velocity of 1.5 km/s and also using a higher migration velocity of 3 km/s. For these cases, the theoretical γ parameter's values are 0.75 and 1.5, respectively.

Using the theoretical values for the parameters, we construct the curves from Al-Yahya, Schleicher and Biloti and our numerical approach and depict the predicted



(a) 10°



(b) 15°

Figure 4: Image gather of the data migrated with an incorrect velocity of 1.5 km/s (left) and 3 km/s (right) at horizontal position 2 km. The red, blue and green dashed lines indicate, respectively, Al-Yahya's, Schleicher and Biloti's and our predicted curve.

curves in the CIGs, see Figures 4 and 5. Here we choose the CIG at position 2 km. In these figures, we window offset and time axes of the images for better visualization.

In Figure 4 (a) and (b), for 10° and 15° dipping reflector, Al-Yahya's proposal presents a little misfit in both cases: lower and higher velocity than the correct migration velocity. Our numerical proposal and Schleicher and Biloti's proposal have similar behavior for higher migration velocity, describing very well the event in the CIG. However, for lower migration velocity, one can observe in Figure 4 (left) an unstable behavior of Schleicher and Biloti's curve for large offset. For instance, in Figure 4(a) this instability happens for offsets beyond 1.2 km.

For increasing dips, we observe that Al-Yahya's curve misfit increases, see Figure 5. This is expected, since Al-Yahya's formula considers only a horizontal reflector. For the reflector of 20° dip, our curve still describes very well the event (Figure 5(a)). The difference between proposals is remarkable for the 25° case, as shows Figure 5(b). For this case, our proposal keeps fitting exactly the event.

With this first experiment, we validate our curve by showing that it describe very well the event. It seems to be much better than the others two proposals. Our curve represents precisely the event in the CIG both as lower as higher

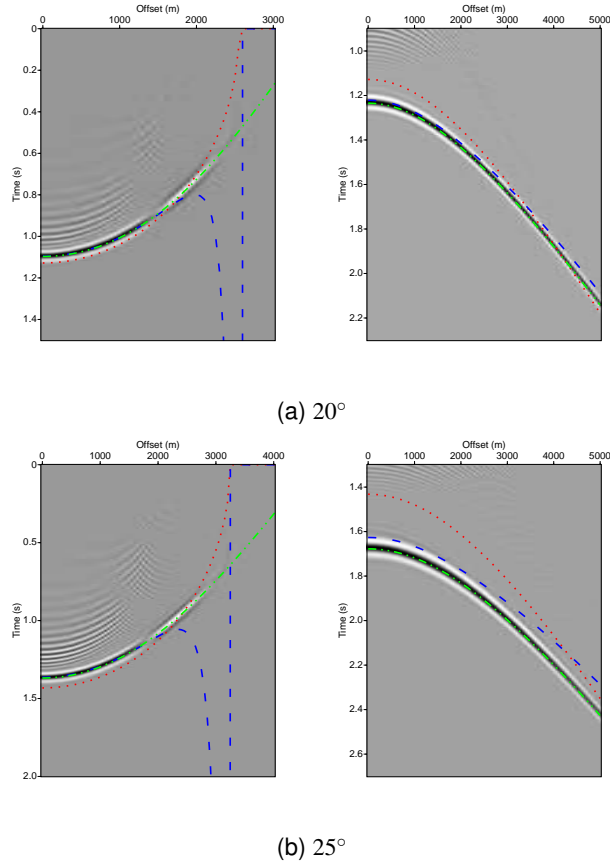


Figure 5: Image gather of the data migrated with an incorrect velocity of 1.5 km/s (left) and 3 km/s (right) at horizontal position 2 km. The red, blue and green dashed lines indicate, respectively, Al-Yahya's, Schleicher and Biloti's and our predicted curve.

migration velocity cases. Furthermore, even for dipping reflector of 25° , our proposal keeps describing very well the event.

Supergathers

For this and next experiment, we added a strong noise of 3 signal-to-noise ratio and Kirchhoff time migrated the data using a migration velocity of 3 km/s.

To analyse the objective function behavior using supergathers, we construct a grid in the velocity correction and the dip related parameters. For each γ and m , we obtain the proposal curve and evaluate the coherence along this curve, as shows Figure 6. Observe that using only one image gather, see Figure 6(a), the theoretical parameters values are not the ones with highest coherence values. It is due to strong noise added to the data. As expected, the use of more image gathers at the same time tend to focus the coherence value, since it intensify the information.

Estimating the parameters

The next step is to test the parameters estimation given by the proposal's curves. In other words, we look for the γ and m parameters whose curves best fit the events. To search those optimal parameters, we apply the BOBYQA method.

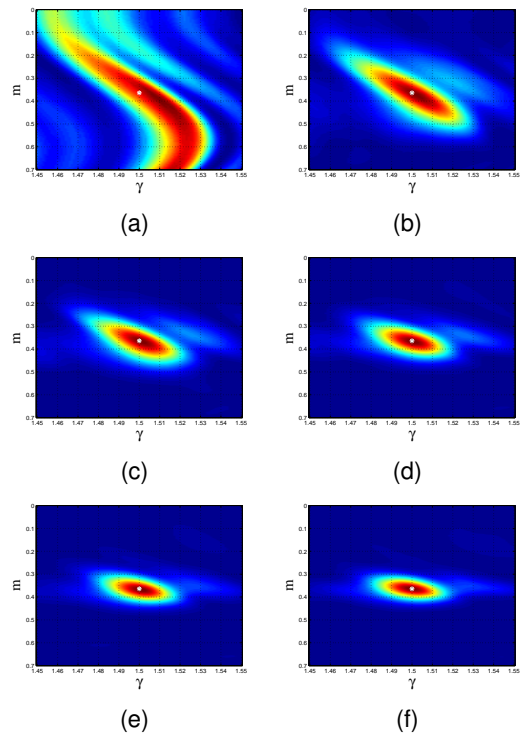


Figure 6: Semblance value for the model of dip 20° for several image gathers, fixing the central image gather at 2 km and using (a) 1, (b) 3, (c) 5, (d) 7, (e) 9 and (f) 11 image gathers. The white cross marks the location of the theoretical parameter values.

To obtain an initial approximation to the optimization method, we construct a coarse grid in the variables γ and m and evaluate the objective function. We choose the values of γ and m that returned the best coherence value as the initial point for the optimization phase.

Given a common image gather, we find parameters associated with the best fitting curves for each time sample. The search procedure is applied to all image gathers. In Figure 7, one vertical line represents the coherence values obtained from the image gather at that position.

Observe that the high coherence path is more defined for our proposal using 1 image gather, Figure 7(c) than for (a) Al-Yahya's and (b) Schleicher and Biloti's proposal. As expected, using more image gathers tend to focus that path, since more information is used to estimate the parameters, as shows Figure 7(d) and (e).

Once obtained the coherence pannel, we search for a high coherence path to extract its associated parameters. The parameters extracted are smoothed by optimal splines Biloti et al. (2003). Figure 8 shows the values of parameter γ extracted over the maximum-coherence paths. To be comparable to Al-Yahya's and Schleicher and Biloti's proposal, we use at this time our proposal only for one image gather. Observe that Al-Yahya's proposals underestimate the velocity correction parameters, since the theoretical value for γ in these cases is 1.5. Our proposal seems to be more stable as increases the dip.

In Figure 9, we compare the results obtained from our

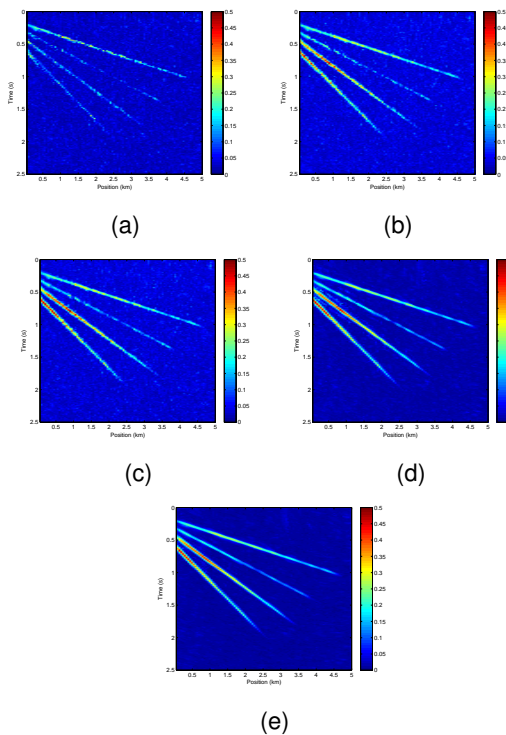


Figure 7: Coherence as obtained from MVA using (a) Al-Yahya, (b) Schleicher and Biloti's and our proposal with (c) 1, (d) 3 and (e) 5 image gathers.

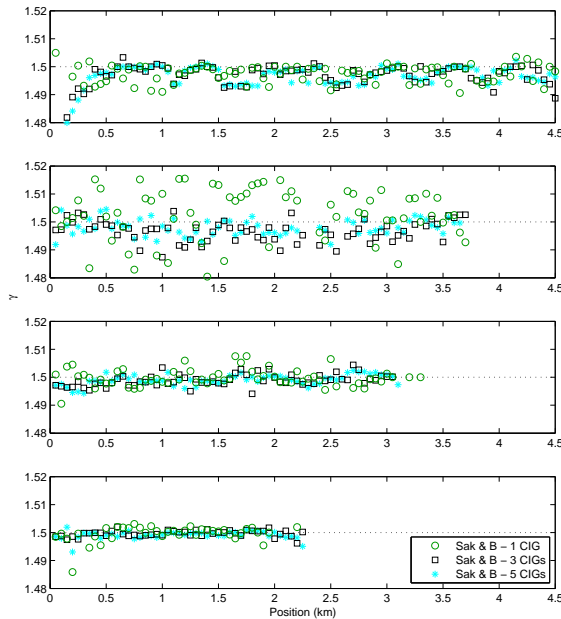


Figure 9: Values of parameter γ obtained from our proposal using 1, 3 and 5 image gathers, from top to bottom, for the first, second, third and fourth reflectors, respectively.

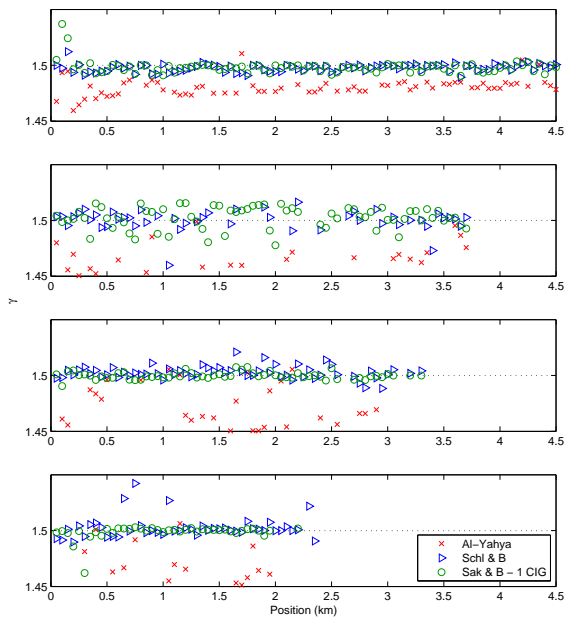


Figure 8: Values of parameter γ obtained from Al-Yahya, Schleicher and Biloti and our proposal, from top to bottom, for the 10°, 15°, 20° and 25° dipping reflectors, respectively.

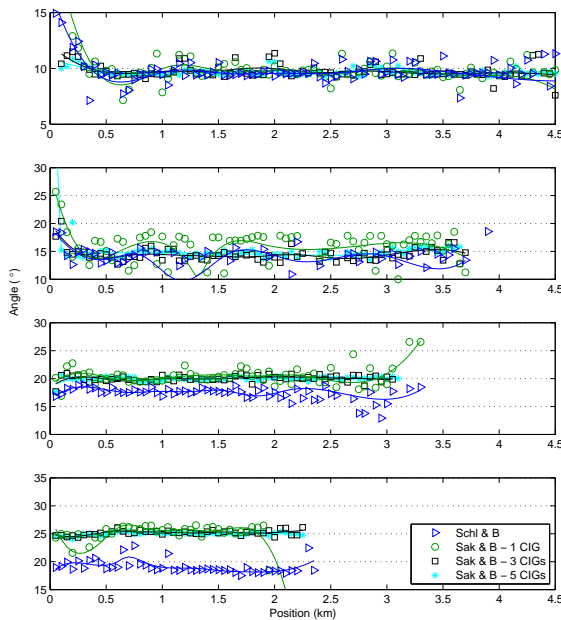


Figure 10: Dip angles obtained from MVA using the Schleicher and Biloti's proposal and our proposal using several image gathers, from top to bottom, for the 10°, 15°, 20° and 25° dipping reflectors, respectively.

proposal using 1, 3 and 5 image gathers to estimate the parameters. It is slightly better γ estimation using more

image gathers. The more accurate is the γ estimation, less velocity fields updates are necessary.

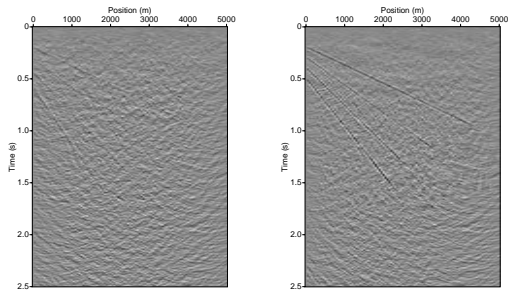


Figure 11: Stack of migrated images using a priori velocity field of 3 km/s(left) and updated velocity using our proposal for 3 image gathers (right).

The dip parameters estimated are showed in Figure 10. For 20° and 25° , Schleicher and Biloti's proposal underestimate the dip parameter. This is evident for the fourth reflector in Figure 10, where their proposal underestimate the reflector dip in about 5° . For all reflectors, our proposal using 5 image gathers better estimates m .

After obtaining the velocity correction parameters, we use them to update the velocity field and migrate the data once again. Along the maximum-coherence path we multiply the gamma obtained with the velocity from the velocity field. Between paths, we fill in the field by linear interpolation of the velocity. Above first path and under last path, the velocity is repeated.

Figure 11 shows the stack of migrated images before and after updating the velocity field using our proposal for 3 image gathers. We omitted the CIG itself to show the flatness because the strong noise make it extremely difficult.

Conclusions

The residual moveout in a common-image gather after migration with an incorrect velocity is governed by a fifth-order polynomial for a dipping reflector case. In this work, we have proposed to solve this polynomial equation numerically to describe the moveout in a coherence-based migration velocity analysis.

We have validated our numerical proposal for the moveout curve and showed that it fits the migrated event better than previously derived approximations from Al-Yahya and Schleicher and Biloti.

A major advantage of our numerical description over the previous approximations is that it allows to extend the residual-moveout analysis to neighbouring image gathers. In this way, more information can be used to determine estimates for the velocity model parameters.

Our numerical experiments demonstrate that the use of a few neighbouring image gathers tend to better define the maximum coherence path, stabilizing and improving the parameter extraction.

Acknowledgements

The authors kindly thank the WIT Consortium Sponsors for the support to this research.

References

- Al-Yahya, K. M. (1989). Velocity analysis by iterative profile migration. *Geophysics*, 54:718–729.
- Biloti, R., Santos, L., and Tygel, M. (2003). Automatic smoothing by optimal splines. *Brazilian Journal of Geophysics*, 21:173–178.
- Powell, M. (2009). The BOBYQA algorithm for bound constrained optimization without derivatives. Technical Report NA 2009/06, University of Cambridge.
- Sattlegger, J. W. (1975). Migration velocity determination: Part I. philosophy. *Geophysics*, 40(1):1–5.
- Schleicher, J. and Biloti, R. (2007). Dip correction for coherence-based time migration velocity analysis. *Geophysics*, 72:S41–S48.
- Stockwell, J. J. W. and Cohen, J. (2008). The new SU (Seismic Unix) User's Manual. *CWP - Colorado School of Mines, USA*.